Ortega, J., Vasconcelos, G., Rodrigues, H., Correia, M., Ferreira, T.M., Vicente, R. Use of post-earthquake damage data to calibrate, validate and compare two seismic vulnerability assessment methods for vernacular architecture. *International Journal of Disaster Risk Reduction* (2019). https://doi.org/10.1016/j.ijdrr.2019.101242

Use of post-earthquake damage data to calibrate, validate and compare two seismic vulnerability assessment methods for vernacular architecture

Javier Ortega[a*], Graça Vasconcelos[a], Hugo Rodrigues[b], Mariana Correia[c], Tiago Miguel Ferreira[a], Romeu Vicente[d]

[a] ISISE, Department of Civil Engineering, University of Minho, Guimarães, Campus de Azurém, 4800-058 Guimarães, Portugal; javier.ortega@civil.uminho.pt (J. Ortega); graca@civil.uminho.pt (G. Vasconcelos); tmferreira@civil.uminho.pt (T.M. Ferreira)

[b] RISCO, School of Technology and Management, Polytechnic Institute of Leiria, Campus 2, 2411-901 Leiria, Portugal; e.mail: hugo.f.rodrigues@ipleiria.pt (H. Rodrigues)

[c] CI-ESG Research Centre, Escola Superior Gallaecia, Vila Nova de Cerveira, Portugal; e.mail: marianacorreia@esg.pt (M. Correia)

[d] University of Aveiro, Aveiro, Portugal; e.mail: romvic@ua.pt (R. Vicente)

* Corresponding author; e-mail: javier.ortega@civil.uminho.pt

Abstract: The paper presents and discusses the application of two large scale seismic vulnerability assessment methods on the island of Faial in Azores (Portugal). The two methods are specifically conceived to assess the seismic vulnerability of vernacular architecture. The first method follows a classical seismic vulnerability index approach and is referred as SVIVA (Seismic Vulnerability Index for Vernacular Architecture). The second method is referred as SAVVAS (Seismic Assessment of the Vulnerability of Vernacular Architecture Structures) and it is a numerical tool intended to estimate the seismic capacity of vernacular buildings in terms of seismic load factors associated with different structural damage limit states. The main reason behind the selection of Faial Island as a case study was the availability of post-earthquake reports of the building stock after the 1998 Azores earthquake, which allowed comparing the damage scenarios obtained using both methods with the post-earthquake damage data and thus helped for the calibration and validation of the two methods. The application of both methods led to a good fit between estimated versus observed damage grades, which validated their applicability as large-scale

first level approaches. Moreover, as the main outcome, the paper presents the novelties of the SAVVAS method, which had not been applied before, and discusses its main advantages, namely: no need for calibration with previous post-earthquake damage data, an enhancement of the prediction capabilities, a more individualized evaluation of the buildings and the possibility to assess the seismic performance of the building in different loading directions.

Keywords: Seismic vulnerability assessment; vernacular architecture; stone masonry; vulnerability index; 1998 Azores earthquake

Acknowledgments

The work presented in this paper was partly financed by FEDER funds through the Competitivity and Internationalization Operational Programme – COMPETE and by national funds through FCT – Foundation for Science and Technology within the scope of the project POC1-01-01-0145-FEDER-007633.

1. Introduction

The increasing vulnerability of vernacular architecture has been already highlighted by different organisms, professionals and scholars (ICOMOS 1999; Degg and Homan 2005; May 2010). The term vernacular commonly applies to non-engineered buildings, typically self-constructed by the owner or the community, based on empirical knowledge and reflecting the tradition and life style of a community, as part of a process that involves many people over many generations. The need for the valorization and the preservation of vernacular architecture has been widely acknowledged because of being a key-element for cultural identity and the fundamental expression of the culture of a community and its relationship with its territory (ICOMOS 1999; Ortega et al. 2017). However, it is nowadays considered in many places as an obsolete way of building and only valued as part of the region's identity (Correia 2017). Typically, people tend to see vernacular construction technologies as unsafe and eventually abandon and substitute them with modern ones. Subsequently, vernacular heritage, along with traditional building knowledge, technologies and materials face the risk of disappearing due to this economic, cultural and architectural homogenization. Moreover, this progressive abandonment increases the vulnerability of vernacular architecture facing natural disasters, including earthquakes.

Seismic vulnerability assessment methods for the built environment can play an important role on mitigating the risk faced by vernacular structures against earthquakes. They are mainly aimed at estimating the damage that a certain structure will suffer as a consequence of a seismic event of a given intensity. In spite of the many seismic vulnerability assessment methods existing in the literature, suitable for different types of analysis and different goals, none has been specifically adapted to the distinct characteristics of vernacular architecture. Based on this gap in knowledge and intending to contribute to the awareness and protection of the vernacular heritage, two novel methods have been previously developed by the authors (Ortega 2018) with vernacular structures as their main target. The methods are particularly focused on the Portuguese vernacular heritage, including stone masonry, fired brick masonry, adobe and earthen constructions, which share many characteristics with other vernacular constructions throughout the world. The present paper intends to evaluate them through a practical application on a set of vernacular buildings in the island of Faial, in Azores (Portugal). These two methods are: (a) Seismic

Vulnerability Index for Vernacular Architecture (SVIVA) method; and (b) Seismic Assessment of the Vulnerability of Vernacular Architecture Structures (SAVVAS) method.

Since both methods aim at the preservation of vernacular architecture, they were conceived as large scale assessments, able to perform analyses comprising a large number of buildings. The built vernacular heritage is rarely represented by single structures, but usually involves a group of buildings and settlements within a rural region or within an historical city center. The two methods are thus first level approaches that can make use of simple more expedite inspections because they can rely on less detailed qualitative information related to a few parameters. This is another crucial matter given the typical lack of resources assigned to the study and preservation of the vernacular heritage. Nevertheless, despite the expedited nature and ease of use of both methods, they should be able to provide a robust estimation of the seismic capacity of vernacular buildings, as well as allow the individual assessment of the buildings.

After the brief introduction of the two methods, the paper presents Faial as the case study. The main objective of the present paper is the calibration and validation of the two new seismic vulnerability assessment methods using a wide set of damage data collected after the 1998 Azores earthquake from Neves et al. (2012) and Ferreira et al. (2017). The data includes information of the existing traditional stone masonry building stock characteristic from the island and the damage survey carried out after the earthquake. The use of post-earthquake damage information allowed the comparison of the damage estimated after the application of the two methods with the observed damage after the earthquake, which led to the calibration and validation of both methods. This exercise was extraordinarily helpful for a better understanding on the use of both methods to perform a seismic vulnerability assessment.

In the end, a detailed discussion of the advantages, drawbacks and limitations of each method is provided, showing a comparison of the performance of both methods. The evaluation of the applicability of the methods for an efficient large-scale seismic vulnerability assessment of vernacular buildings is considered as the main contribution of the paper, since both methods had not been applied before. As a conclusion, the paper discusses the potential of both methods to contribute to the preservation of the built vernacular heritage located in earthquake prone areas by evaluating the reliability of the methods in predicting damage to vernacular buildings. The paper also focuses on evaluating the capability of the methods to identify the most vulnerable elements at risk and

possible weaknesses and failure mechanisms of the building, which is particularly important because they can eventually allow defining and assessing appropriate structural retrofitting strategies at an urban or regional level as evidenced by Ferreira et al. (2017b).

2. Overview of the two evaluated seismic vulnerability assessment methods

The main components of seismic vulnerability assessment methods are vulnerability curves of functions that express the probability of a building to suffer a certain degree of damage according to the earthquake ground motion severity. Seismic vulnerability assessment methods can be generally classified into four general categories according to the approach followed to extract correlations between damage and ground motion: (a) empirical methods are defined on the basis of post-earthquake damage data; (b) analytical methods define vulnerability functions on the basis of analytical and numerical studies; (c) expert-based methods rely on expert judgment; and (d) some methods can be classified as hybrid, since they result from a combined use of the previously described approaches.

Simplified seismic vulnerability assessment approaches aimed at large scale analyses are typically empirical methods, relying on qualitative data gathered from post-earthquake damage observation. Correlations between damage and seismic motion are defined for different building typologies after observing the damage suffered due to a particular earthquake (Calvi et al. 2006). Even though there exist a great number of empirical vulnerability functions in the literature developed from post-earthquake damage data, there is a large variation in the procedures applied to collect the data (e.g. damage characterization, data quality, etc.) or in the selected ground motion intensity (Rossetto et al 2015). There are also different ways of expressing this relationship. For instance, damage probability matrices (DPM) can be formulated in a discrete form based on the concept that a particular structural typology has a similar probability of reaching a given damage state after an earthquake of a given intensity. They were firstly proposed by Whitman et al. (1973), based on the damage caused by the 1971 San Fernando earthquake. Afterward, more DPM were developed after the occurrence of different earthquakes, using different intensity and damage scales (Braga et al. 1982; Grünthal 1998; Doce et al. 2003; Di Pasquale et al. 2005; Eleftheriadou and Karabinis 2011). Another possibility of describing the damage-motion relationship is through continuous vulnerability functions, first developed by Spence et al. (1992). The main problem to overcome for

their derivation is that both earthquake intensity and damage are typically expressed in a discrete form and not as continuous variables. However, different authors used different ways to describe the earthquake action and the damage in order to develop empirical vulnerability or fragility curves after post-earthquake surveys (Sabetta et al. 1998; Rota et al. 2006; Colombi et al 2008; Azizi-bondarabadi et al 2016). Empirical methods require a large set of post-earthquake damage data which is usually not available. Moreover, the obtained empirical correlations cannot always be extrapolated to other scenarios with a different building stock. Nonetheless, they are adequate for large scale analyses because they use simple qualitative data that can be obtained from an expedite evaluation of the buildings. Another important limitation of these methods is the difficulty of associating the damage observed to a single seismic event, since they are not able to take into account damage accumulation induced by the subsequent occurrence of aftershock earthquakes (Hofer et al 2018).

Analytical methods use models representing buildings or building components and perform structural analysis to evaluate the seismic effect on the structures, in terms of damage. There are many methods that can range different degrees of complexity depending on the type of model selected to simulate the structure and the analytical procedure adopted to perform the analyses. Analytical vulnerability curves can then be derived through regression analysis on the damage distribution data obtained after performing a large number of analyses on the models. Some common analytical methods existing in the literature are based on simplified mechanical models and limit state analysis (Calvi 1999) or kinematic limit analysis (D'Ayala and Speranza 2003; Zampieri et al 2016). Others make use of more sophisticated models and nonlinear static analysis procedures (ATC-40 1996; Fajfar 1999). Many recent studies use the equivalent frame model (Lagomarsino et al. 2013) and perform a high number of nonlinear dynamic and static analyses in order to obtain vulnerability curves for different masonry building typologies (Erberick 2008; Pasticier et al. 2008; Rota et al. 2010). Analytical approaches are suitable to overcome the lack of post-earthquake damage observations, but they require more detailed information and a better understanding of construction details and materials to prepare the models. Thus, they can be very computationally expensive to use on large-scale analysis comprising areas with buildings showing diverse construction characteristics. Moreover, they highly depend on the analytical model considered. For example, some of the mentioned equivalent frame models disregard the out-of-plane behavior of the walls, which is a common failure mechanism for unreinforced masonry buildings. Another important limitation is the simulation of the ground

motion and, in the case of dynamic analysis, the record selection, which highly influences the results of the seismic vulnerability assessment (Zanini et al 2018). On the other hand, the use of complex numerical modeling also allows taking into account the effect of constructive and material characteristics that cannot be typically considered in empirical methods, meaning that it is an appropriate tool to carry out parametric studies. It is noted that analytical methods should be always validated with empirical observations.

Expert-based methods emerged as a result of the limited post-earthquake damage data in terms of different building typologies and the high costs related to analytical approaches (Jaiswal et al. 2012). On the basis of expert opinion and previous knowledge, these methods estimate the damage that a certain structure can suffer for a given seismic intensity by analyzing the structural characteristics of the constructions and classifying them into different building typologies (ATC-13 1985; HAZUS 1999). Finally, there are also hybrid methods that result from a combined use of the previously described approaches, such as the vulnerability index method (Benedetti and Petrini 1984) and the macroseismic method (Lagomarsino and Giovinazzi 2006), which are supported by statistical studies of post-earthquake damage information, but also rely on expert opinion.

This brief overview of existing seismic vulnerability assessment methods in the literature shows that recent works have applied analytical approaches to derive fragility and vulnerability functions for different building types and structures (D'Ayala et al. 2014; Pitilakis et al. 2014; Zampieri et al. 2016; Silva et al. 2019). However, these approaches have not been applied to vernacular masonry or earthen structures. Accurate numerical models with nonlinear material constitutive laws have not been yet applied to develop specific vulnerability assessment methods for vernacular buildings. This gap in knowledge and the need to support traditional methods with analytical and numerical studies was therefore detected. The two methods evaluated and applied in the present paper have been developed specifically for vernacular architecture using an analytical approach instead of an empirical one. This process included an extensive numerical parametric study based on detailed finite element modeling and nonlinear static (pushover) analysis intended to quantify the influence of a set of geometrical, structural, constructive and material parameters in the seismic response of vernacular buildings. A brief overview of the two seismic vulnerability assessment methods under evaluation is provided next, but the reader is referred to Ortega (2018) for an in-depth explanation of their development.

2.1. The SVIVA method

The SVIVA method proposes a new formulation for the classical vulnerability index approach, firstly proposed by Benedetti and Petrini (1984), adapted to the characteristics of vernacular architecture. Ultimately, it consists of an adaptation of the hybrid approach followed by Vicente (2008), which combines the vulnerability index method and the macroseismic method proposed by Giovinazzi and Lagomarsino (2004). These approaches are all based on empirical post-earthquake damage observation and expert opinion. In the case of the SVIVA formulation, the quantification of each parameter's influence on the seismic behavior of vernacular buildings, which resulted in an updated definition of the parameters' classes and weights were defined based on the previously mentioned extensive numerical parametric campaign (Ortega 2018).

Vulnerability index methods provide a measure of the building vulnerability under seismic loads through a dimensionless vulnerability index (I_V) (Barbat et al. 1996). Table 1 shows the SVIVA vulnerability index formulation for vernacular architecture. As shown schematically in Figure 1, the method is composed of ten vulnerability parameters, which were selected based on existing vulnerability index formulations described in the literature (Sepe et al. 2008; Boukri and Bensaibi 2008; Vicente et al. 2011; Ferreira et al. 2014; Shakya 2014) and on the earthquake performance of vernacular constructions observed in past earthquakes (Blondet et al. 2011; Bothara et al. 2012; Neves et al. 2012; Sorrentino et al. 2013; Gautam et al. 2016).

Each building is evaluated by providing a vulnerability class for each of them. Four seismic vulnerability classes of increasing vulnerability, from A (lowest) to D (highest), are defined for each parameter and associated with a qualification coefficient (C_{vi}). Following the common vulnerability index formulations existing in the literature, the qualification coefficients are the same for all parameters. Class A is related to the lowest vulnerability class coefficient ($C_{vi} = 0$), while class D is related to the highest vulnerability class coefficient ($C_{vi} = 50$). It should be noted that they have not been calibrated. The calibration with the post-observation data takes effect over the weights assigned to the parameters. This is intended to provide a formulation that is similar to those existing in the literature and results in vulnerability index values within a similar range. Thus, results can be comparable. Each parameter is also associated to a weight (p_i), reflecting its relative importance and ranging from 0.5 for the least important to 1.5 for the most important ones. The vulnerability index (I_V) is calculated as the weighted sum

of ten parameters using the equation shown in Table 1. The value of I_V ranges between 0 and 500 but, it is common, for ease of use, to normalize it to fall within a range between 0 (very low vulnerability) and 100 (very high).

Table 1. SVIVA vulnerability index formulation

Parameter	Class (C_{vi}) A	B	C	D	Weight (p_i)	Vulnerability index
P1. Wall slenderness	0	5	20	50	1.00	
P2. Maximum wall span	0	5	20	50	0.50	$I_V = \sum_{i=1}^{10} C_{vi} \times p_i$
P3. Type of material	0	5	20	50	1.50	
P4. Wall-to-wall connections	0	5	20	50	0.75	
P5. Horizontal diaphragms	0	5	20	50	1.50	$0 \leq I_V \leq 500$
P6. Roof thrust	0	5	20	50	0.50	
P7. Wall openings	0	5	20	50	1.50	
P8. Number of floors	0	5	20	50	1.50	Normalized index
P9. State of conservation	0	5	20	50	0.75	$0 \leq I_V \leq 100$
P10. In-plane index	0	5	20	50	0.50	

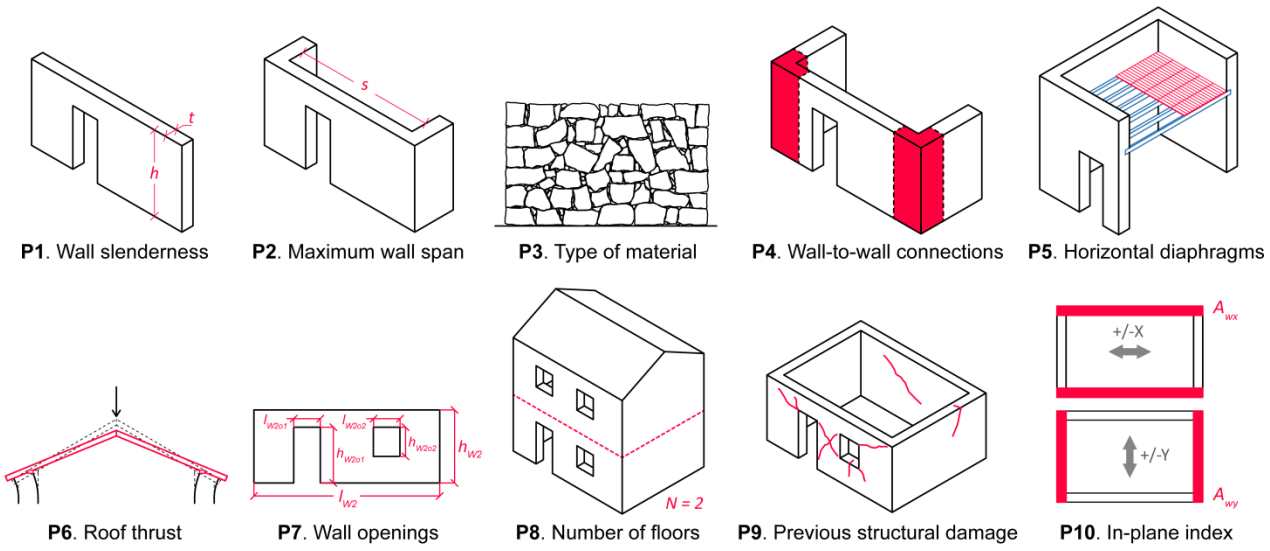

Figure 1. Seismic vulnerability assessment parameters considered for the SVIVA and SAVVAS methods

The strategy of the parametric study used to define the parameters classes consisted of modifying a reference numerical model according to the different parameters. Nonlinear static (pushover) analyses were carried out for all the models constructed. The variations on the seismic performance according to the variations in the parameters could be thus analyzed and quantified. This procedure led to the definition of the seismic vulnerability classes. The definition of the parameters weight was carried out by using statistical analysis. The results of the parametric

study were assembled into a database. Multiple linear regression analysis led to assess the relative importance of the different parameters in defining the seismic performance of the buildings analyzed.

Performing a seismic vulnerability assessment requires an expression that is able to correlate the estimated vulnerability index of the building (I_V) with the expected damage to be suffered for different seismic inputs. As previously stated, the SVIVA method follows the approach defined by Vicente (2008). Therefore, it uses the analytical expression from the macroseismic method developed by Giovinazzi and Lagomarsino (2004):

$$\mu_D = 2.5\left[1 + tanh\left(\frac{\mathrm{I} + aV - b}{Q}\right)\right] \quad (1)$$

where *I* is the seismic input in terms of macroseismic intensity, *V* is the vulnerability index and *Q* is the ductility index, which is an empirically defined index that takes into account the ductility of a determined construction typology, typically ranging from 1 to 4 (Vicente et al. 2011). Coefficients *a* and *b* should be calibrated for the set of buildings under analysis when post-earthquake damage data is available. This analytical expression can be used to build vulnerability curves for the subsequent seismic vulnerability evaluation and estimation of losses. It should be noted that the vulnerability indexes used by the vulnerability index method (I_v) and the macroseismic method (*V*) are different. Thus, following the procedure described by Vicente (2008), I_V had to be transformed into the vulnerability index used in the macroseismic method (*V*), using another analytical correlation:

$$\mathrm{V} = c + d \times I_V \quad (2)$$

where *c* and *d* are again coefficients that can be calibrated for the type of buildings under evaluation based on post-earthquake observations. The calibrating procedure for all coefficients *a*, *b*, *c* and *d* using existing earthquake damage surveys is presented in section 4.1.

2.2. SAVVAS method

The SAVVAS method also makes use of a set of parameters related to geometrical, structural, constructive and material characteristics of vernacular buildings shown in Figure 1. However, this novel approach intends to estimate the maximum seismic capacity of buildings in quantitative terms. The results of the extensive numerical parametric analysis carried out to evaluate and quantify the influence of these parameters on the seismic response

of vernacular buildings were compiled into a database (Ortega 2018). Regression analysis was performed on the database to extract correlations between the seismic capacity of the building and the key parameters shown in Figure 1. As a result, the SAVVAS method is a numerical tool consisting of different formulations that allow defining the seismic capacity of the building through seismic load factors expressed as accelerations (in terms of g) associated with different structural damage limit states, using as input simple variables based on the ten key seismic vulnerability assessment parameters. Thus, the SAVVAS method is intended to be an analytical approach developed using numerical and statistical analysis.

The SAVVAS formulation and procedure is shown in Table 2. The first step of the SAVVAS method is partially common to the SVIVA method, namely the assignment of seismic vulnerability classes to the parameters. However, as shown in Table 2, while some of the parameters are defined by assigning a seismic vulnerability class from 1 to 4, directly associated to the classification from A to D defined also for the SVIVA method, others had to be defined through specifying different quantitative attributes. For example, P2 (maximum wall span) can be directly defined by the span (in m), instead of by the vulnerability class. The same occurs for P1, defined by the wall slenderness ratio ($\lambda = h/t$) and P8, defined by the number of floors (N) of the building. P10 refers to the in-plane index (γ_i) and it is also defined quantitatively as the ratio between the in-plane area of earthquake resistant walls in each main direction (A_{wi}) and the total in-plane area of the earthquake resistant walls (A_w): $\gamma_i = A_{wi}/A_w$. Parameter P7 refers to the amount and area of walls openings and was further divided into two parameters, aiming at distinguishing between: (1) *P7a*, ratio between the maximum area of openings in the walls perpendicular to the loading direction and the total surface area of the walls; and (2) *P7b*, ratio between the area of wall openings in all in-plane resisting walls and the total surface area of all in-plane resisting walls. The remaining parameters, including the type of material (P3), the quality of the wall-to-wall connections (P4), the horizontal diaphragms (P5), the roof thrust (P6) and the previous structural damage (P9), are defined as a function of their class, in qualitative terms. Thus, they are described in a discrete form, assuming four countable numbers from 1 to 4.

Table 2. SAVVAS formulation and procedure

Step 1	**Definition of the seismic vulnerability assessment parameters**									
	P1	**P2**	**P3**	**P4**	**P5**	**P6**	**P7**		**P8**	**P9**	**P10**
	λ	s	*P3 [1-4]*	*P4 [1-4]*	*P5 [1-4]*	*P6 [1-4]*	*P7a*	*P7b*	N	*P9 [1-4]*	γ_i
Step 2	**Calculation of the load factors associated to the limit states in each main direction *i* (in terms of *g*)**										
	$$\boldsymbol{LS1_i = e^{(1.97-0.06\lambda-0.1s-0.68\ln(P3)-0.14P4-0.28P5-0.39\ln(P6)-3.43P7b-0.82\ln(N)-2.27\ln(P9)+0.63P5P7b)} - c}$$										
	$$\boldsymbol{LS2_i = 0.16 \times LS1(g) + 0.78 \times LS3(g)}$$										
	$$\boldsymbol{LS3_i = e^{(2.16-0.04\lambda-0.05s-0.24P3-0.16P4-0.28P5-0.08P6+0.3P7a-2.79P7b-0.37N-0.15P9+0.74\gamma_i+0.44P5P7b)}}$$										
Step 3	**Calculation of the global load factors defining the limit states of the building (in terms of *g*)**										
	$$\boldsymbol{LS1 = \min(LS1_i)}$$										
	$$\boldsymbol{LS2 = \min(LS2_i)}$$										
	$$\boldsymbol{LS3 = \min(LS3_i)}$$										

With respect to the load factors defining the structural limit states (LS1, LS2 and LS3), they are associated to specific damage levels exhibited by the structure. They were determined according to the pushover (capacity) curves obtained from the parametric analyses, which is a relation between the load factor (ratio between the horizontal forces at the base and the self-weight of the structure) and the displacement at a control node (taken as the node where the highest displacements occur), see Figure 2. They provide information of both load and deformation capacity of the building, in terms of stiffness and ductility. Nevertheless, the basis of comparison of the seismic capacity of the SAVVAS method is defined in terms of load capacity. Therefore, the limit states are established according to the seismic actions that can cause the building to reach the different structural limit states. They are expressed as an acceleration (in terms of *g*). LS1 can be associated to an Immediate Occupancy Limit State. Before this limit, the structural behavior of the building remains in the elastic branch and the structure can be considered as fully operational. LS1 thus corresponds to the formation of the first cracks in the structure, characterizing the end of the elastic response. LS2 is associated to a Damage Limitation Limit State, as it depicts the transition between a point where the structure is still functional, retaining most of its original stiffness and strength, showing minor structural damage and cracks, and a state where significant damage is visible so that the building could not be used after without significant repair. LS3 can be referred as Life Safety Limit State and is defined by the load factor and displacement corresponding to the attainment of the building maximum resistance. As a result, the building has lost a significant amount of its original stiffness, but is supposed to retain some lateral

strength and, in the case of masonry structures, they still may show a large margin against collapse in terms of displacements. Nevertheless, they should not be used after the earthquake. It is noted that LS4 is associated to the Near Collapse Limit State, but was excluded because it corresponds to the point where the building maximum strength is reduced 20%, thus being mathematically dependent on LS3. The load factor associated to the collapse of the building is thus not defined according to the pushover curve and was calibrated in a subsequent step using post-earthquake damage data (see Section 4.2.).

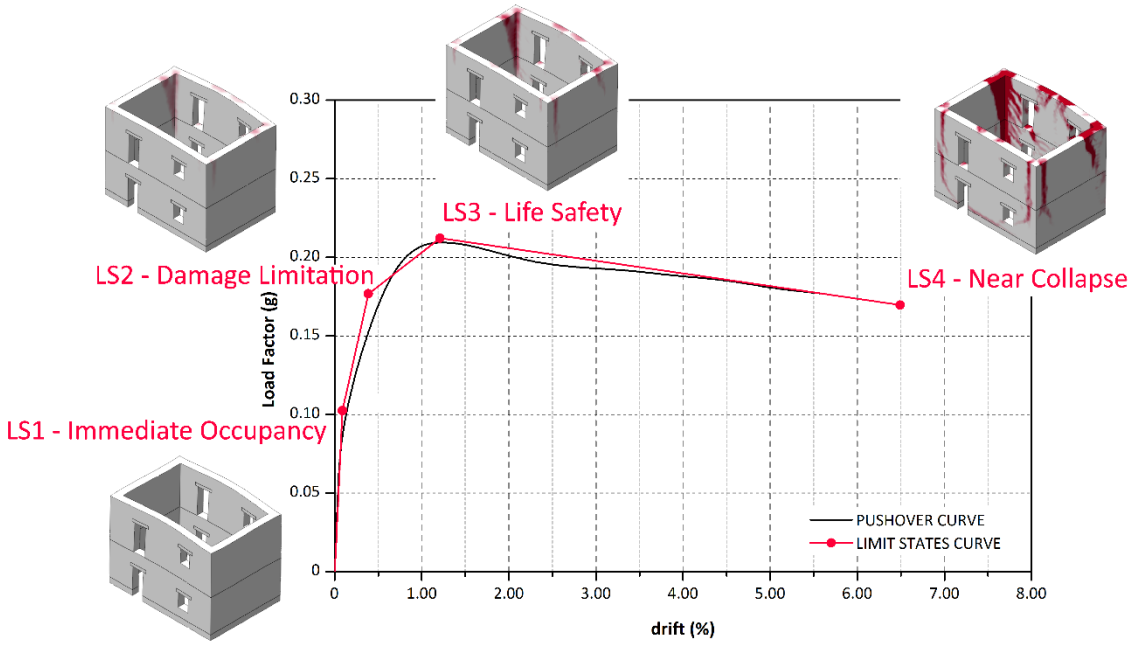

Figure 2. Definition of the limit states according to the pushover curve

The expressions from Step 2 of the SAVVAS formulation that allow calculating the load factors were obtained from the multiple linear regression analysis performed on the database. These regression models obtained showed a good correlation between the seismic capacity of the building and the ten key parameters selected (Ortega 2018). It should be also noted that the load factors can be calculated for the four main directions of the building (+/-X and +/-Y). This is intended to provide a more accurate description and understanding of the seismic behavior of the evaluated vernacular buildings, as well as a better estimation of their most vulnerable direction. However, in order to have a global seismic assessment of the building, the minimum values for each LS obtained among the four resisting directions are given as the global load factors defining the seismic vulnerability of the building. This is the last step of the procedure and, as a result, the SAVVAS method provides an estimation of the minimum

load that will cause the building to reach the different limit states. Since the load factors related with the different structural damage limit states are expressed as accelerations, they can be used in a straightforward way to eventually correlate the seismic action in terms of peak ground acceleration (PGA) with the expected damage.

3. Damage data after the 1998 Azores earthquake

The 1998 Azores earthquake struck the central group of the Azores Archipelago with a moment magnitude $M_w = 6.2$, mainly striking Faial, Pico and San Jorge islands. The earthquake reached high levels of destruction and affected more than 5000 people, causing 8 fatalities and leaving 1500 persons homeless (Matias et al. 2007). A Modified Mercalli Intensity (MMI) scale distribution map for the Faial Island was proposed by Zonno et al. (2010) based on post-earthquake damage survey campaigns, see Figure 3. Nevertheless, it is noted that the construction of this document is subjected to uncertainties and Zonno et al. (2010) argues that some locations might have been subjected to higher intensities than those plotted on the map.

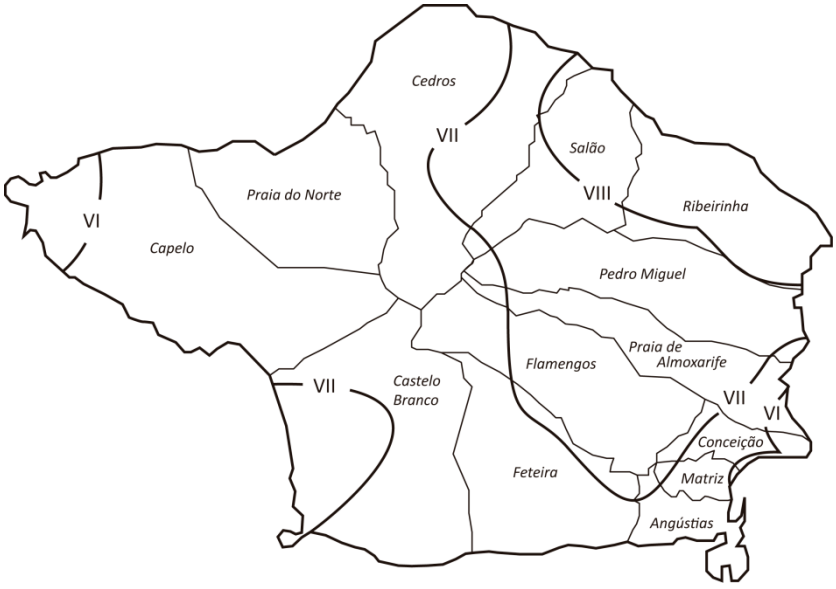

Figure 3. MMI scale distribution map of Faial Island indicating the administrative subdivision of the island into the different districts (adapted from Ferreira et al. (2017a))

3.1. Building stock characterization

The seismic event was followed by the collection of extensive data on the effects of the earthquake on the building stock of the islands. Neves et al. (2012) focused on the detailed characterization of the buildings in the Faial Island

and particularly presented a detailed study of the construction systems that characterize the traditional architecture of the island, whose structure is mainly composed of stone masonry load bearing walls, timber floor diaphragms and timber roof trusses. This is particularly adequate, given that the two seismic vulnerability assessment methods proposed are mainly addressed for this structural typology. Neves et al. (2012) also proposed a detailed damage classification for this traditional masonry building stock by identifying the main damage patterns surveyed. Moreover, the earthquake also attracted a significant amount of scientific research dedicated to the characterization of the mechanical properties of the traditional construction techniques from the island (Costa 2002; Costa et al. 2011; Costa et al. 2013). This vast amount of information gathered and produced on the seismic performance of traditional Azorean masonry constructions after the 1998 earthquake makes this case study very appropriate for the calibration of the two seismic vulnerability assessment methods proposed. Actually, it has also been previously used to calibrate other seismic vulnerability assessments methods (Neves et al. 2012; Ferreira et al. 2017a).

The same set of 88 masonry buildings used by Ferreira et al. (2017a) was also selected for the application and calibration of the two methods proposed in this work. This selection includes comprehensive information on different representative traditional masonry construction types scattered throughout various villages in Faial Island. Both rural and urban building types are present in the selection, see Figure 4. The reader is referred to Costa and Arêde (2006) and Neves et al. (2012) for a more detailed description of these buildings in terms of construction systems and materials. The documentation available for each of these 88 buildings varied widely: from very detailed reports drafted during the reconstruction process with information of the original and retrofitted structure (including plans, damage reports and photographs) to very limited information with barely a damage report fulfilled on-site or a couple of photographs.

Figure 4. Examples of typical traditional Azorean masonry construction types in the island of Faial present in the selection: (a) one-floor rural building; (b) two-floor rural building; and (c) three-floor urban building

3.2. Damage classification

A general damage distribution of 3,154 traditional masonry buildings on Faial and Pico Islands was presented in Neves et al. (2012). The set of 88 buildings in Faial selected for this study was meant to include buildings presenting a wide variation in terms of the observed grade of damage. The classification of the damage observed in each building was carried out according to the EMS-98 European Macroseismic Scale (Grünthal 1998) and is presented in Table 3 as a reference. This damage classification was chosen because the macroseismic method (Giovinazzi and Lagomarsino 2004) is based on the EMS-98 macroseismic scale defined by Grünthal (1998). Thus, the mean damage grade (μ_D) estimated using this approach directly relates to the classification shown in Table 3. The same damage grade is also the main output of the SAVVAS method, allowing the direct comparison between the results obtained using both methods.

The buildings were thus classified in terms of damage using the data available. It is worth noting that a damage assessment is always subjective and depends on the judgment of the evaluator. Besides, as previously stated, the existing information on the buildings is variable and, in some cases, limited. Therefore, in order to minimize uncertainties and to have a more robust and reliable assessment, four experts carried out the evaluation of the damage grades for the 88 buildings independently. The results were then analyzed and compared. The final damage classification adopted for each building was the mean value obtained from the four evaluations. This approach also provided the opportunity of obtaining mid-values in between the 6 damage grades (e.g. 3.25), which

allowed a better comparison with the damage values resulting from the two seismic vulnerability assessment methods that express damage as a continuous variable.

Table 3. Damage grades adopted for the study based on the EMS-98 (Grünthal 1998)

Damage grade		Description
0	No damage	No observed damage
1	Negligible to slight damage	No structural damage and/or slight non-structural damage: hairline cracks in very few walls, fall of small pieces of plaster, fall or loose stones from upper parts of buildings in very few cases
2	Moderate damage	Slight structural damage and/or moderate non-structural damage: cracks in many walls, fall of large pieces of plaster, partial collapse of chimneys
3	Substantial to heavy damage	Moderate structural damage and/or heavy non-structural damage: large and extensive cracks in most walls, roof tiles detach, chimneys fracture at the roof line, failure of individual non-structural elements (partition or gable walls)
4	Very heavy damage	Heavy structural damage and/or very heavy non-structural damage: serious failure of walls, partial structural failure of roofs and floors
5	Destruction	Very heavy structural damage: total or near total collapse

Figure 5 shows several examples of buildings classified under the five damage grades. None of the buildings in the set was considered as grade 0, since all of them presented at least slight non-structural damage. The examples are compared with reference drawing provided by the EMS-98 scale. Figure 6 shows the distribution of the assessed buildings according to their estimated damage level. Damage levels in the graph are used as thresholds and include all buildings that have not reached the following damage level (i.e. buildings whose damage grade was estimated as 3.5 are included within damage grade 3). The graph shows that the majority of the buildings (over 65%) did not reach damage grade 3 and, thus, did not present substantial structural damage.

356

357 Figure 5. Examples of evaluated buildings belonging to each damage grade from the EMS-98 scale

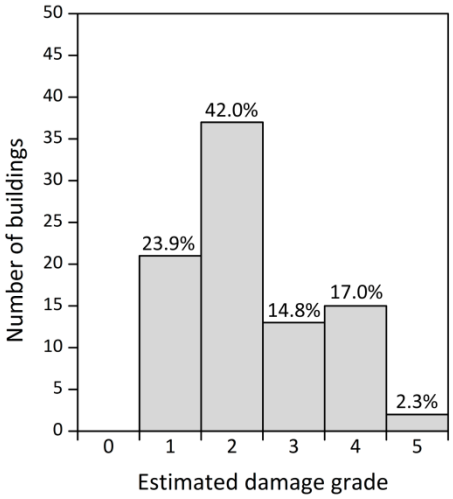

Figure 6. Distribution of the evaluated buildings according to the estimated damage grade

4. Calibration and validation of the methods

As previously mentioned, both seismic vulnerability assessment methods that are evaluated in the present paper make use of geometrical, structural, constructive and material parameters to estimate the building vulnerability. Thus, the parameter survey (i.e. classification of each parameter in terms of seismic vulnerability class or quantitative attribute) is a crucial step for the application of the two proposed methods. It is worth highlighting that, just as with the damage classification, the damage data available for each building is not always complete enough to carry out a sound parameter survey. Therefore, some assumptions had to be made in order to decide the class for some of the parameters. The parameter survey is much dependent on the qualitative judgment of the person conducting the assessment, since different persons may reach to different classifications.

The definition of the classes can be particularly difficult for parameters that are not easily evaluated from the exterior, such as the quality of the wall-to-wall connections or the type of horizontal diaphragm. In this particular case, for example, it should be also noted that interpreting the class for parameter P9, which refers to the previous structural damage in the building, was very difficult, since all the pictures available correspond to the state of the buildings after the earthquake. Thus, it was decided to establish that all buildings fell within class A for parameter P9, so that this parameter does not have a relative influence in the results. As abovementioned, the information available for some of the buildings barely consisted of a brief damage report and a couple of photographs. For

these buildings with limited information, the data obtained from other buildings from the set with more detailed information served as the basis for extrapolation. Also, the detailed construction characterization of the masonry walls, timber roofs and timber floors, conducted by Neves et al. (2012), was very helpful for the determination of some parameters classes.

4.1. Seismic Vulnerability Index for Vernacular Architecture (SVIVA) method

The application of the formulation to the 88 buildings from Faial resulted in the vulnerability index distribution presented in Figure 7. The mean value of the seismic vulnerability index (I_V) obtained is 43.22 with a standard deviation value (STD) of 7.1, which results in a coefficient of variation (CoV) of 16%. The minimum and maximum values of I_V are 21.5 and 55 respectively. The little variation within the index shows clearly that most of the buildings assessed belong to similar construction typologies. The main typological difference occurs between the rural and urban buildings. However, even between both construction types, the majority of the classification of the parameters coincides.

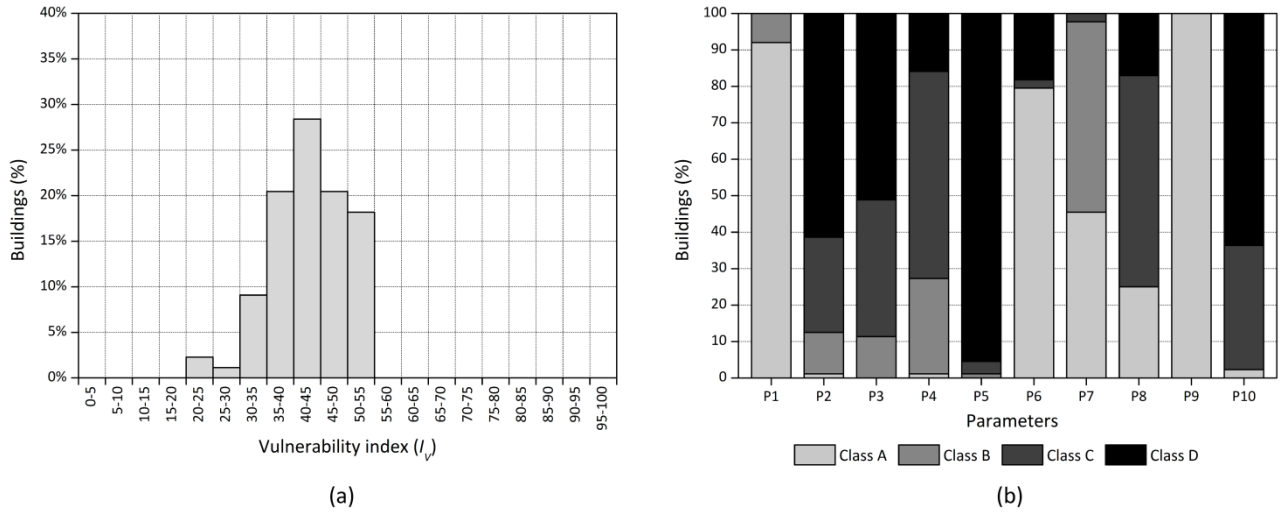

Figure 7. (a) Vulnerability index (I_V) distribution; and (b) parameter class distribution

The expected mean damage grade (μ_D) can be estimated for each building using Eq. 1, as a function of the building vulnerability and the seismic input. It is noted that μ_D also refers to the damage classification from EMS-98 shown in Table 3. Thus, the results obtained can be compared with the observed damage level on the buildings after the earthquake (Figure 6). The buildings were grouped by location and intensity, following the district subdivision

shown in the intensity map (Figure 3). The seismic input (*I*) from Eq. 1 is also expressed in terms of the EMS-98. Following the recommendations of Musson et al. (2010), the degrees from the MMI scale depicted in the intensity map from Figure 3 can be directly correlated with the degrees from the EMS-98 scale, acknowledging a certain degree of subjectivity involved within this assumption (Ferreira et al. 2017), Thus, a scale V in MMI scale can be associated to a scale V in the EMS-98 scale.

The initial mean damage grade estimated using the original formulation and the coefficients proposed by Vicente (2008), where *a*, *b*, *c*, *d* and *Q* were 6.25, 12.7, 0.56, 0.0064 and 3 respectively, did not match well the observed results (Figure 8). Therefore, a curve-fitting process was applied in order to find a better approximation between the observed damage-vulnerability index point cloud and the vulnerability curves. Thus, Eq. 1 and Eq. 2 had to be calibrated for the buildings under analysis. The availability of post-earthquake damage data allows the comparison between the estimated and the observed damage. The fitting process was carried out using CurveExpert Pro software (Hyams 2017). This software automatizes the process of finding the best fit allowing the definition of a custom regression model based on the analytical expressions shown in Eq. 1 and Eq. 2. Subsequently, these two analytical expressions could be calibrated to better represent the seismic behavior observed for this particular type of buildings, by means of varying the coefficients that define both expressions. The resulting calibrated expressions are shown below, highlighting in bold the updated coefficients:

$$\mu_D = 2.5\left[1 + tanh\left(\frac{\mathrm{I} + 6.25V - 12.7}{Q}\right)\right] \tag{3}$$

$$\mathrm{V} = 0.46 + 0.012 \times I_V \tag{4}$$

The ductility index (*Q*) is empirical parameter and depends on the construction typology evaluated. In this study, a value of 2.0 is assumed based on recommendations of other authors dealing with load bearing masonry wall construction types (Ferreira et al. 2017a; Shakya 2014). This factor defines the slope of the vulnerability curve and the value of 2.0 adopted also proved to provide the most accurate approximation. The fitting process resulted in a significant improvement in the correlation between the estimated and observed damage. Figure 8 shows side by side plots of the mean damage grade observed (μ_D) versus the vulnerability index (I_V), with the corresponding vulnerability curves built using the original formulation and the calibrated one, for the three different macroseismic intensities registered in the island (*VI*, *VII* and *VIII*). It should be noted that, since only a few

buildings within the set correspond to areas where the macroseismic intensity level registered was VIII, the improvement resulting from the fitting process is less optimized (Figure 8c). The significant differences between both curves illustrate the inherent uncertainty of these formulations to estimate damage, since they depend on parameters that can only be calibrated with post-earthquake damage data. This fact also highlights the importance of interpreting the results statistically and in comparative terms, as a first-level assessment that highlights those buildings that are more vulnerable than others and require further more detailed evaluation. With regard to the partial distributions of I_V for each intensity level, a mean value of 41.1, 46.1 and 41.2 were obtained for $I_{EMS-98} = VI, VII$ and $VIII$, respectively. The similar values obtained confirmed a construction typology homogeneity of the set of buildings evaluated and showed that the fact that some buildings suffered a higher level of damage should be associated to the higher accelerations registered in those areas.

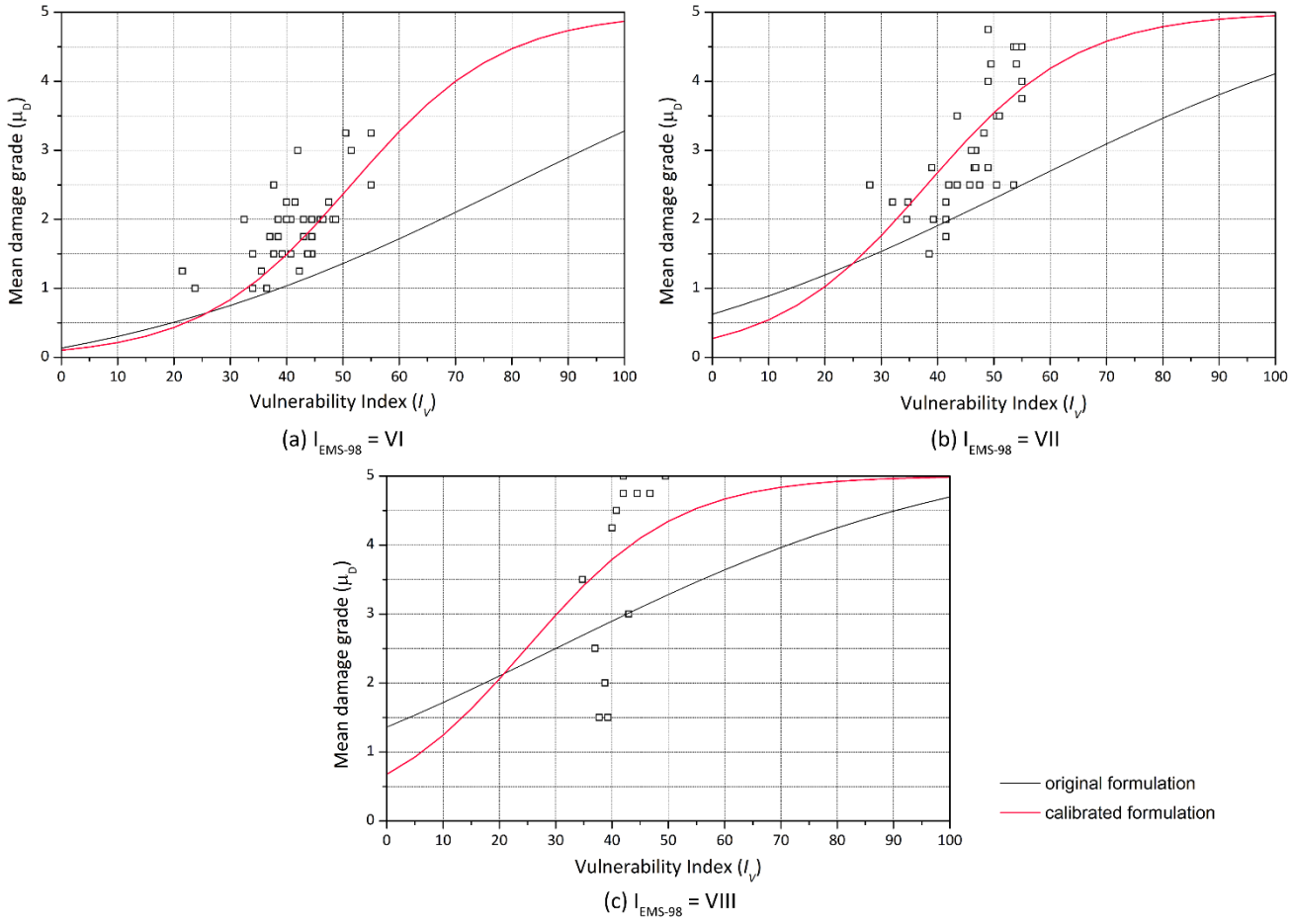

Figure 8. Observed damage versus mean damage grade estimated using the original and updated expressions for the construction of the vulnerability curves, grouped by the different macrosesimic intensities

The damage estimation achieved using this new proposed vulnerability index formulation was considered satisfactory. The estimated versus observed damage plot is shown in Figure 9a, while Figure 9b presents the residual versus observed damage. The value of the coefficient of determination (R^2) obtained reaches 0.605. This coefficient measures how well the model fits the actual data. A value of 0.605 can be considered high for these simplified seismic vulnerability assessment methods. The errors are also low, showing a maximum error in the prediction of 2.24, but a Mean Absolute Error (MAE) value of 0.56 and a Root-Mean-Squared Error (RMSE) value of 0.71. The graph from Figure 9b shows that the level of damage is predicted within a maximum difference of 1 level for the great majority of the buildings, with the exception of a few cases. Acknowledging the uncertainties inherent to the whole prediction process, namely the attribution of the macroseismic intensities, the assignment of a level of damage and the selection of the parameter classes to the different buildings, it should be highlighted that the results show a good prediction capability. The model is able to recognize the most vulnerable constructions and provide a good estimate of the damage that each building might suffer for earthquakes of different intensities.

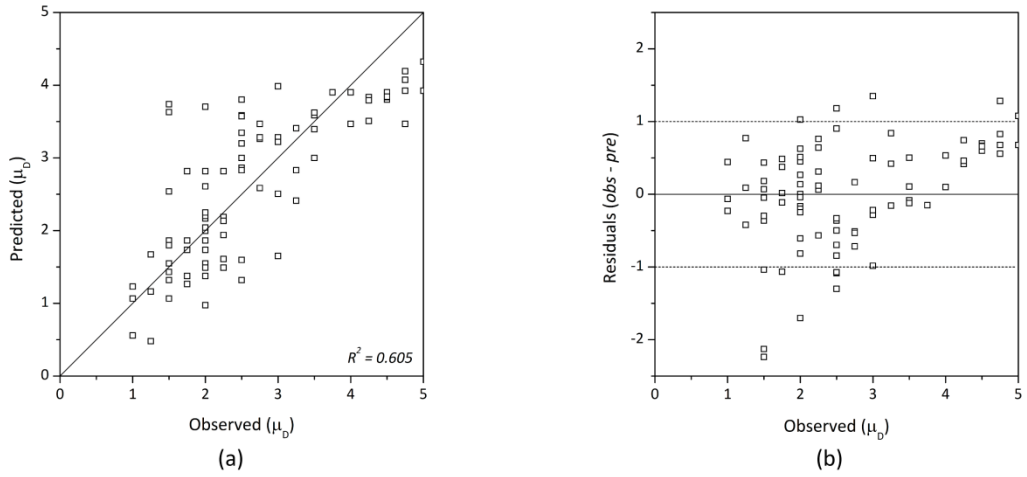

Figure 9. (a) Predicted versus observed damage grades; and (b) residuals versus observed damage grades

4.2. Seismic Assessment of the Vulnerability of Vernacular Architecture Structures (SAVVAS) method

The SAVVAS method was applied on the same 88 buildings, following procedure specified in Table 2 and leading to the load factor distributions shown in Figure 10. The mean values of the load factors obtained are 0.13g, 0.22g

and 0.25g for LS1, LS2 and LS3 respectively, with a standard deviation (STD) value of 0.06g, 0.08g and 0.09g, which result in coefficients of variation (CoV) of 47%, 37% and 36%. These results show significantly greater variations than the ones obtained from the vulnerability index method, which suggests that the SAVVAS method is able to distinguish the capacity of the buildings that previously had the same vulnerability index (I_V). Therefore, the SAVVAS method seems to be able to detect more precisely the differences in the seismic performance of the different buildings, even though they belong to a very similar construction typology. It is noted that a detailed comparison between the results obtained using both methods is provided later.

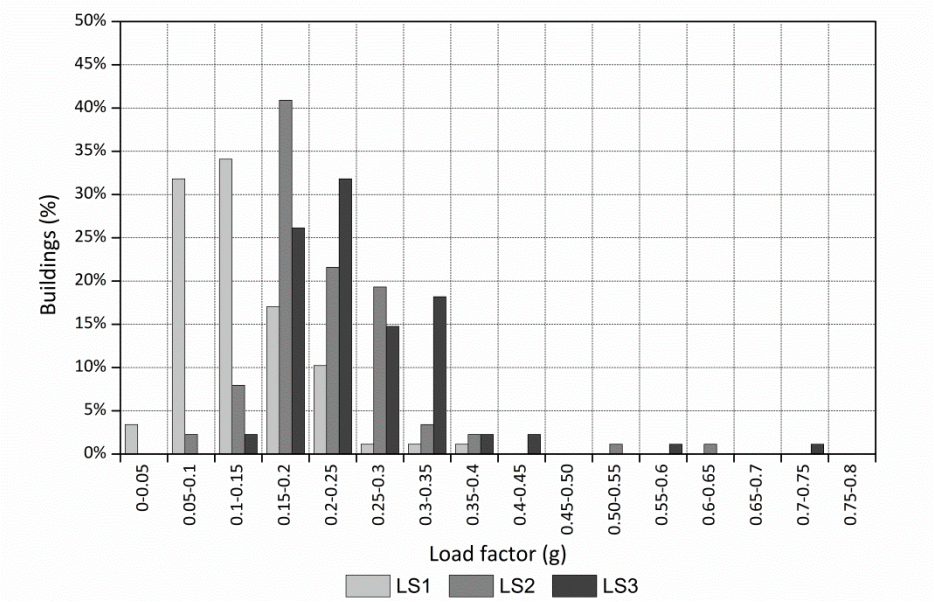

Figure 10. Load factor distributions for the three limit states: LS1, LS2 and LS3

A first seismic assessment of the buildings can be carried out just by comparing the seismic load factors obtained with the seismic demand established by the code. For Faial Island, the value of reference peak ground acceleration (PGA) is 0.25g (NP EN1998-1 2010). About 60% of the buildings present a load factor corresponding to LS3 below 0.25g, which means that their maximum capacity would be exceeded by the design load action of an earthquake with the characteristics defined by the code. This is a first indicator that reveals the vulnerability of the buildings in the island. Moreover, most of the buildings are prone to suffer structural damage. For 95% of the buildings evaluated, the load factor corresponding to LS1 obtained is considerably lower than 0.25g (Figure 10).

Table 4 shows the statistics obtained for the vulnerability parameters corresponding to the surveyed buildings. Table 4 also includes the statistics from the computed global load factors defining the three limit states. Similarly

to what we could observe in Figure 7, the variations found for some parameters are very small, particularly for parameters P1 (wall slenderness), P3 (type of material) and P5 (horizontal diaphragms). Therefore, the majority of the buildings belong to a similar construction type that consists of thick load bearing irregular masonry walls with flexible timber horizontal diaphragms. The higher deviation shown by the remaining parameters can be attributed to: (a) the parameters are classified differently for each main direction; and (b) parameters are more specifically classified and have a wider range of variation. For example, the variation observed for parameter P6 is due to the fact that, within the same building, some walls might be considered to receive the roof thrust while others do not. This is common when buildings have gable roofs (as is the case for most of the buildings under analysis), where only two walls can receive the possible thrust from the roof. Regarding parameter P2, walls get to span distances over 15 m in several cases, which also confirms a clear trend for the buildings in the island to be very slender in plan ($\gamma_i > 0.75$). The coefficient of variation (CoV) for the two parameters addressing wall openings is very high because of the low value of the mean. However, the buildings typically present few openings, with some exception of those located in urban areas, which can show facades with up to 49% of wall openings. With respect to the number of floors, there is also a greater variation, which is associated mainly to the fact that many buildings are built in a slope. Therefore, different sides of the buildings can present different heights, which results also different values for this parameter within the same building.

Table 4. Statistics from the parametric survey and the estimated load factors defining each limit state

Variables		Units	Minimum	Maximum	Mean	Median	Mode	STD	CoV (%)
Parameters	**P1**	λ	3.71	7.07	5.12	5.00	5.38	0.64	12.33
	P2	m	2.85	17.40	7.38	6.52	4.50	3.30	44.74
	P3	*Class*	2	4	3.47	4	4	0.66	19.04
	P4	*Class*	1	4	2.90	3	3	0.67	23.00
	P5	*Class*	2	4	3.68	4	4	0.49	13.42
	P6	*Class*	1	4	1.33	1	1	0.92	69.43
	P7a	*P7a*	0	0.49	0.09	0.06	0	0.10	110.64
	P7b	*P7b*	0	0.36	0.07	0.06	0	0.06	96.43
	P8	*N*	1	3	1.49	1	1	0.63	42.08
	P9	*Class*	1	1	1	1	1	0	0.00
	P10	γ_i	0.19	0.71	0.39	0.40	0.45	0.10	24.34
Load factor	**LS1**	g	0.04	0.38	0.13	0.12	-	0.06	46.67
	LS2	g	0.09	0.63	0.22	0.20	-	0.08	36.72
	LS3	g	0.11	0.74	0.25	0.23	-	0.09	36.13

As abovementioned, it should be here noted that in cases where there is a limited amount of information available, some of the values assigned to each parameter had to be inferred from a reduced set of pictures. The conditions observed in other buildings with more detailed information served as reference. However, there was no way to know if, for example, there were intermediate resisting walls that can reduce the span value adopted for P2 or, if the condition of the wall-to-wall connections was good. For these buildings, the analysis of the damage developed during the earthquake helped also to infer the classification of some of the parameters, taking into account that the damage is typically associated to deficiencies of the building. As an example, some photographs depicted the collapse of some walls allow detecting deficient wall-to-wall connections otherwise impossible to detect by a visual survey from the outside of the building, see Figure 11.

Figure 11. Examples of collapsed buildings showing deficient wall-to-wall connections

The use of the real post-earthquake damage information available from the 1998 Azores earthquake was in fact very useful to gain knowledge on how to carry out the parameter survey. The classification of some parameters was not straightforward in many cases. Some assumptions were considered in the present work that can be helpful for the future application of the method, including: (1) the wall slenderness might vary among the different walls of the building, the minimum observed was considered for all directions; (2) whenever walls showed different number of floors along their length because of being constructed in a slope, the maximum height was always considered; or (3) the value of the in-plane index considered in all directions was always the minimum calculated, unless the building presents a class A or B type of diaphragm (P5), able to redistribute the load to the earthquake resistant walls in the loading direction. These assumptions were always aimed at taking into account the worst scenario.

The next step after the application of the SAVVAS method consists of the estimation of damage grade based on the EMS-98 scale, correlated with the calculated load factors associated to the three limit states defined. In a first step, the SAVVAS method requires that the seismic input is expressed in terms of PGA instead of macroseismic intensity, so that it can be compared with the values of load factor. The existing data for the 1998 earthquake included strong-motion records and a large collection of post-earthquake damage in the building stock. Based on this information, Zonno et al. (2010) prepared possible PGA maps for the earthquake, according to two possible epicenter locations (Figure 12), but stated that the second epicenter considered (Figure 12b) best reproduced the observed effects of the Faial earthquake.

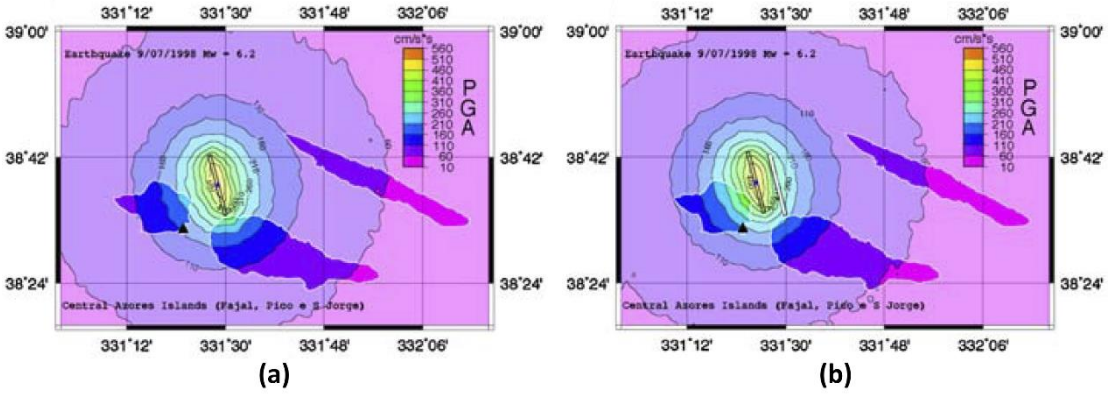

Figure 12. PGA maps computed by Zonno et al. (2010) for the 1998 Azores earthquake assuming two different possible epicenters

The previously shown MMI map (Figure 3) used for the application of the SVIVA method was constructed based on the surveyed damage data, as abovementioned. Subsequently, in order to have comparable results, the PGA values could be inferred from the values of MMI shown in the map. There are many empirical relationships between seismic intensity and acceleration. These expressions are typically derived based on data from previous earthquakes in different locations and the macroseismic intensity is correlated with the logarithm of the ground shaking parameter (such as the PGA). Table 5 shows some correlation relationships between macroseismic intensity and PGA existing in the literature, as well as the results obtained when applied to the MMI map from Figure 3. None of these expressions were derived based on previous earthquake data from Azores and all lead to different values of PGA, showing significant scatter, clearly illustrated by the high coefficient of variation (CoV) shown in the table. Therefore, there is a great amount of subjectivity of adopting one expression on top of another

for the present study. As a result, this study adopts as a reference the PGA map computed by Zonno et al. (2010) using the epicenter that fitted best the damage observed after 1998 Faial earthquake (Figure 12b).

After the definition of the seismic input, a correlation between seismic input, load factors (expressed in g) associated to the structural limit states and mean damage grade (μ_D) has to be defined. Results need to be expressed in terms of the same EMS-98 damage grade scale in order to enable the output of the SAVVAS method to be comparable with other seismic vulnerability assessment methods, such as the macroseismic method. Figure 13 shows the equivalence between the structural limit states defined from the pushover curve and EMS-98 damage grades.

Table 5. Intensity-PGA relationships from the literature

Reference	Correlation	PGA (g)		
		I = VI	*I = VII*	*I = VIII*
Murphy and O'Brien (1977)	$\boldsymbol{log(PGA) = 0.25 + 0.25I_{MM}}$	0.06	0.10	0.18
Guagenti and Petrini (1989)	$\boldsymbol{log(PGA) = 0.602I - 7.073}$	0.03	0.06	0.10
Margotini et al. (1992)	$\boldsymbol{PGA = 0.003353 \times 10^{0.2201 \times I_{MSK}}}$	0.07	0.12	0.19
Theodulis and Papazachos (1992)	$\boldsymbol{log(PGA) = 0.28 + 0.67I_{MM}}$	0.11	0.22	0.44
Decanini et al. (1995)	$\boldsymbol{log(PGA) = 0.594 + 0.237I_{MM}}$	0.11	0.18	0.32
Wald et al. (1999)	$\boldsymbol{I_{MM} = 3.66 \times log(PGA) - 1.66}$	0.13	0.24	0.44
Marin et al. (2004)	$\boldsymbol{I_{MM} = 10 + 2.3 \times log(PGA)}$	0.02	0.05	0.14
Faccioli and Cauzzi (2006)	$\boldsymbol{I_{MCS} = 1.96 \times log(PGA) + 6.54}$	0.05	0.18	0.57
Gómez Capera et al. (2007)	$\boldsymbol{log(PGA) = -1.33 + 0.20I_{MCS}}$	0.08	0.12	0.19
Tselentis and Danciu (2008)	$\boldsymbol{I_{MM} = -0.946 + 3.563 \times log(PGA)}$	0.09	0.17	0.33
Bilal and Askan (2014)	$\boldsymbol{I_{MM} = 0.132 + 3.884 \times log(PGA)}$	0.03	0.06	0.11
Gómez Capera et al. (2015)	$\boldsymbol{I_{MCS} = -0.64 + 3.58 \times log(PGA)}$	0.07	0.14	0.26
Zanini et al. (2019)	$\boldsymbol{I_{EMS-98} = 2.03 + 2.28 \times log(PGA)}$	0.06	0.15	0.42
	Mean (CoV)	0.07 (48%)	0.14 (44%)	0.28 (52%)

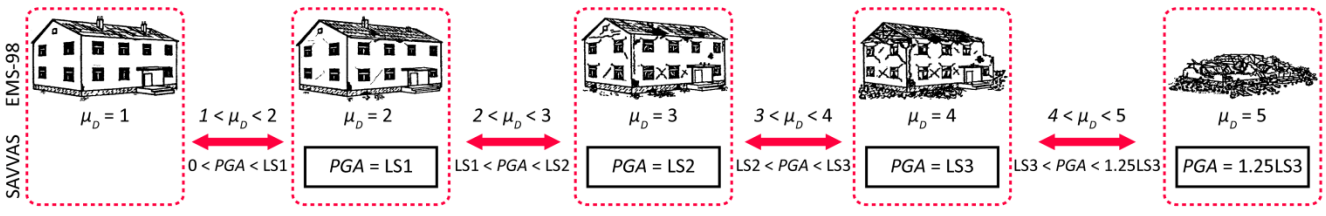

Figure 13. Correlation between the seismic input (PGA), SAVVAS limit states and EMS-98 damage grades

Figure 13 shows that damage grade 0 was removed from the scale. The SAVVAS method does not detect non-structural damage. Grades 0 and 1 are the same and represent the starting point of the scale representing no

structural damage. The load factor defining LS1 delimits the point where the building reaches damage grade 2 and, thus, for values of PGA higher than LS1, the building is assumed to start presenting slight structural damage. Similarly, LS2 is associated to damage grade 3 and LS3 with damage grade 4. The correlation with the 5th damage grade that refers to the total or near collapse of the structure was not straightforward. An empirical factor was established to define a load that would cause the collapse of the building and could be related to damage grade 5. This factor was calibrated using the damage data from the 1998 earthquake to fit better the collapse observed and was finally set as 1.25 times the value found for LS3. The final damage values for the ranges of PGA between limit states are obtained from simple linear interpolation in order to provide a continuous variable.

Once this correlation was established, the level of damage was assessed for the 88 buildings evaluated. The estimation of damage achieved using the SAVVAS method was deemed considerably accurate, clearly outperforming the prediction capability of the SVIVA method. Figure 14a gives the estimated versus observed damage plot, while Figure 14b presents the residual versus observed damage. The value of R^2 obtained from the correlation between observed and predicted damage reaches 0.802 and was considered quite satisfactory. The errors are also reduced, showing a maximum error in the prediction of 2.33 but a MAE of 0.32 and a RMSE of 0.71. The graph from Figure 14b shows that the level of damage is predicted within a maximum difference of less than 0.5 in the damage level for the great majority of the buildings.

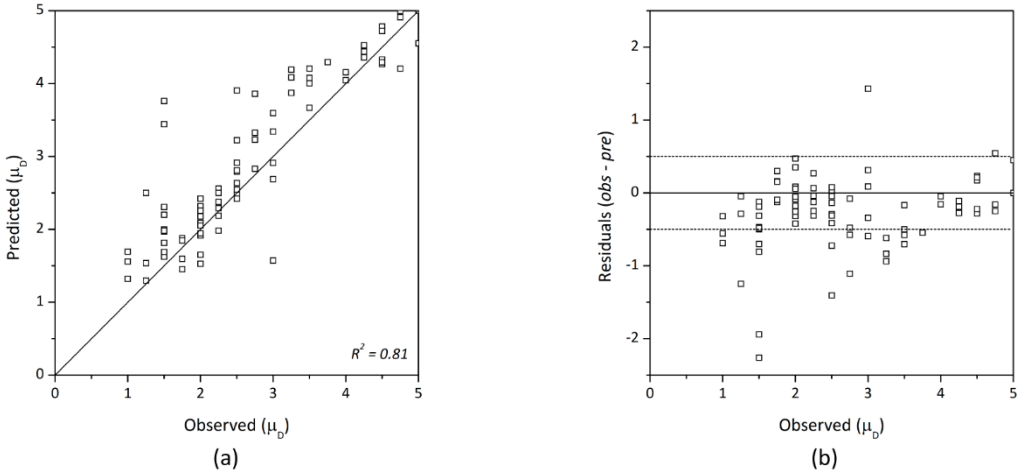

Figure 14. (a) Predicted versus observed damage grades; and (b) residuals versus observed damage grades

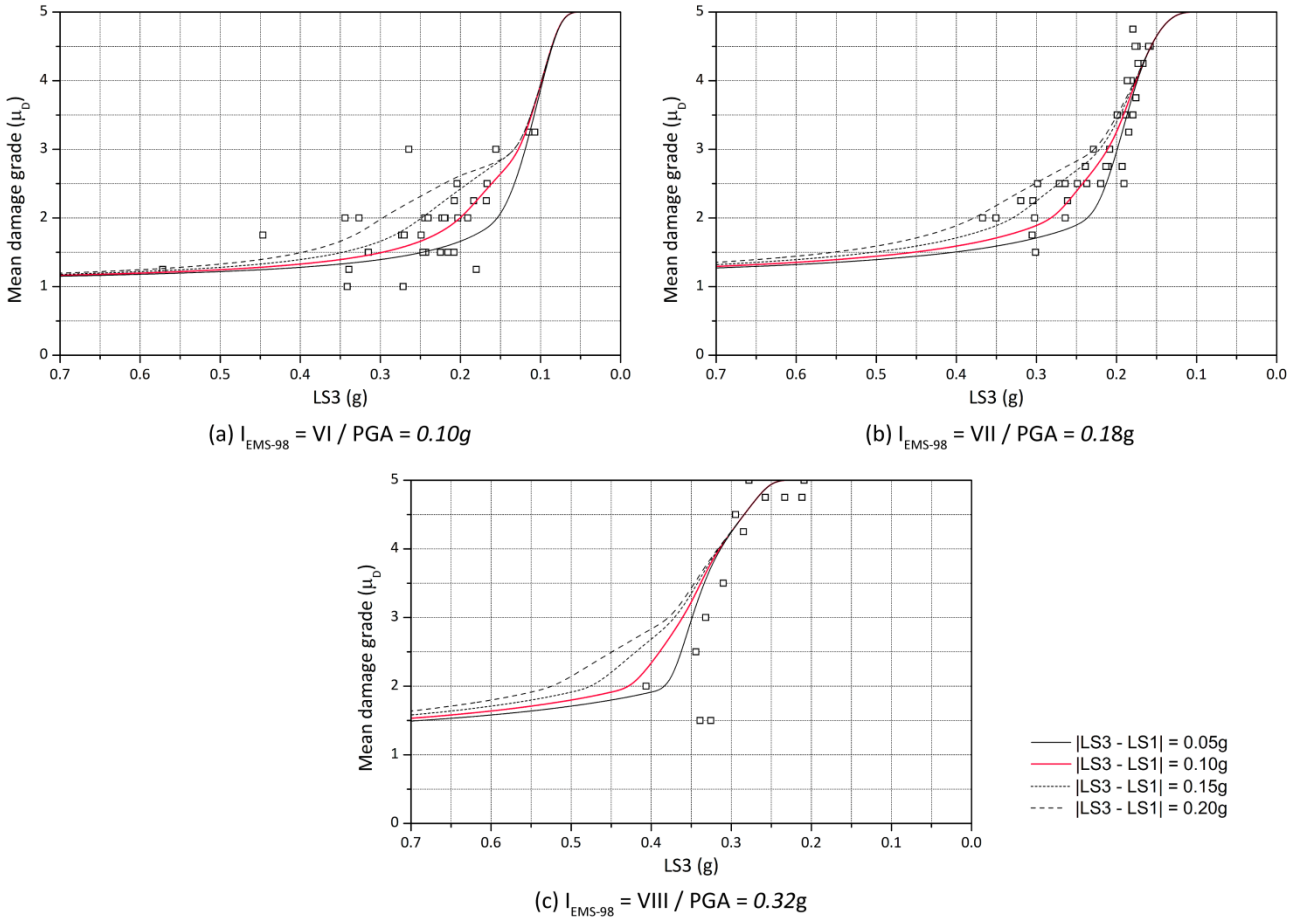

Figure 15. Observed damage versus mean damage grade estimated using the SAVVAS method for the construction of the vulnerability curves as a function of LS3, grouped by the different *PGA*

4.3. Comparison between the two methods

Both seismic vulnerability assessment methods are evidently related since they are based on the same parameters and were developed on the basis of a numerical parametric study (Ortega 2018). The classes of the parameters are also common to both methods. Thus, a strong correlation between the vulnerability index (I_V) obtained with the SVIVA method and the load factors obtained with the SAVVAS method can be observed. Figure 16 shows the correlation between the vulnerability index and the load factor corresponding to LS3 ($I_V - LS3$), as an example. However, it is noted that the SAVVAS method allows a more detailed seismic vulnerability assessment. The estimation of the numerical load factors based on numerical values adopted for the definition of some parameters enables to have a greater variation on the load factors when compared with the vulnerability index. Figure 16 shows clearly that, for some buildings with the same vulnerability index, the load factor defining LS3 estimated

571 with the SAVVAS method varies greatly. For instance there is a building with $I_V = 39$ and $LS3 = 0.21g$ and
572 buildings with $I_V = 39$ and $LS3 = 0.41g$. In this particular example, for the same vulnerability index, the
573 predicted maximum capacity of the building almost doubles. This example highlights the capability of the
574 SAVVAS method to provide more detailed results.

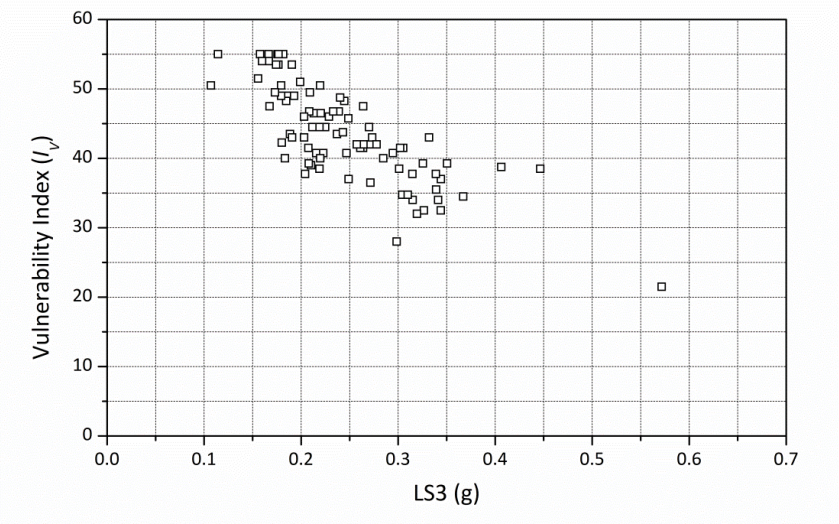

575

576 Figure 16. Correlation between vulnerability index (I_V) and *LS3(g)*

577 The more detailed seismic vulnerability assessment obtained from the SAVVAS method results in a commonly
578 higher accuracy in the prediction of damage, as previously reported, showing also a significant reduction of the
579 deviation with respect to the damage observed (Figure 17). Besides, the requirement of numerical values does not
580 generate an increment in the complexity of the application of the technique, since the parameters are defined by
581 simple ratios that are usually also required for the definition of the classes for the vulnerability index method. It
582 should be noted that in addition to the higher value of R^2 obtained, results are reliable because of the low errors
583 obtained (MAE of 0.32) and the fact that there is not a systematic underestimation or overestimation of the damage
584 observed (Figure 14b).

585 Another main advantage of the SAVVAS method is the fact that it does not require the calibration of the
586 vulnerability curves performed for the SVIVA method. The coefficients from the expression defined by the
587 macroseismic method (Eq. 1) had to be redefined based on the observed damage in order to establish Eq. 3 and
588 Eq. 4. As shown during the assessment performed (Figure 8), the discrepancies can be quite high from using the
589 original formulation and the calibrated ones. This is an important limitation when performing a seismic

vulnerability assessment where an initial calibration is not possible. The SAVVAS method was in this sense applied blindly and provided good results from the beginning. In this method, just the factor of 1.25 defining the damage grade associated to the collapse of the building was calibrated, but its definition does not have such an influence on the results, since it only affects one level **of** the damage scale. In fact, the definition of the collapse is acknowledged as the main weakness of the SAVVAS method. Only the limit states LS1-LS3 are defined according to an extensive numerical parametric study (Ortega 2018). The last damage grade has been here defined using this empirically devised factor of 1.25 that has been validated using this case study. Further research on the definition of the collapse for the SAVVAS method is recommended.

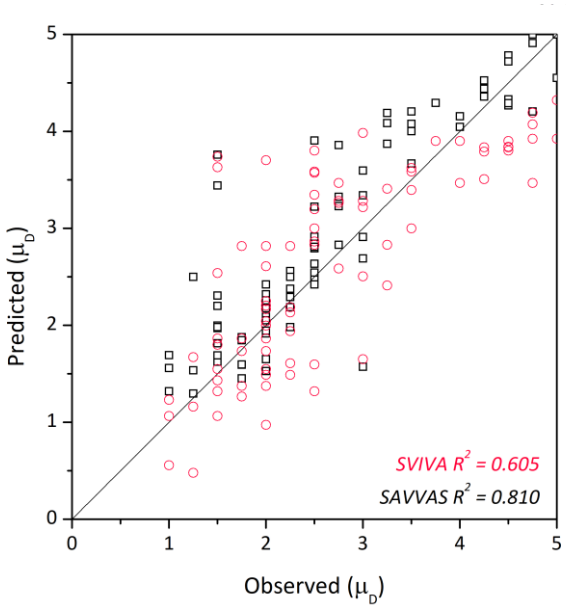

Figure 17. Comparison between predicted and observed damage grades obtained with the SVIVA vulnerability index method and the SAVVAS method evaluated

Another main difference among the SAVVAS and the SVIVA method concerns the seismic input. While the SVIVA method requires the definition of an earthquake scenario in terms of general macroseismic intensities, the SAVVAS method is carried out using values of PGA to define the seismic event. In the case study presented, the PGA scenario used is based on an already defined MMI scenario. However, this does not necessarily have to be always the case. A more detailed scenario can be defined based, for example, on the seismic microzonation of the area under study, which takes into account local effects. Therefore, the seismic vulnerability assessment can be carried out on the basis of more detailed seismic hazard scenarios. Moreover, using the site response spectra and

estimating the building natural frequency, the assessment can be carried out using specific accelerations adapted to each building and site. Further research is also recommended continuing with this research line.

In any case, besides these aspects related to the damage prediction potential of both methods, the biggest advantage of this type of seismic vulnerability assessment methods lies in their ability to detect possible deficiencies and strengths on the building stock under evaluation. Results are therefore particularly valuable in comparative terms, as they offer an expeditious and reliable evaluation on the buildings that are more vulnerable within a set, which is very useful to define and address structural retrofitting strategies at a regional or urban level.

Regarding this latter aspect, one advantage of the SAVVAS method is that this method allows evaluating the seismic load factors of the building in the four main directions of the building. Therefore, when carrying out the seismic vulnerability assessment, results did not only show a good correlation in terms of global damage, but were also able in many cases to identify the failure mode suffered by the building, as the most vulnerable direction identified matched the collapse observed at the earthquake. The evaluation of one building from the dataset is shown below as an example. Figure 18 shows the building plan and exterior and interior views depicting the damage suffered. Since the plans of the building were available, the quantitative parameters could be properly identified, leaving some uncertainty only for the classification of the qualitative parameters, namely the quality of the wall-to-wall connection (P4), type of material (P3), level of roof thrust (P6) and previous structural damage (P9). This case had sufficiently detailed data to fulfill the parameter survey easily, see Table 6. Besides the good correlation between the damage predicted and observed, the method is able to detect that the most vulnerable direction is +Y direction, which involves the gable wall that actually collapsed in reality (Table 6). The building also suffered damage at the connection between the walls at the interior. The method also predicts that the building is prone to suffer structural damage for low values of acceleration ($LS1 = 0.14g$), matching the damage observed.

Figure 18. (a) Building plan and directions nomenclature; (b) main façade of the building; (c) collapsed gable wall; and (d) visible damage at the wall-to-wall connections from the interior of the building

Table 6. Parameter survey and results obtained per main resisting direction (*PGA* = 0.18g)

		Variables														Damage	
Method	**Dir.**	**P1**	**P2**	**P3**	**P4**	**P5**	**P6**	**P7a**	**P7b**	**P8**	**P9**	**P10**	**LS1**	**LS2**	**LS3**	**Predicted**	**Observed**
SAVVAS	+X	4.79	12.99	4	4	3	1	0.03	0.02	1	1	0.29	0.14	0.19	0.22	4.02	3.75
	-X	4,79	12.99	4	4	3	1	0.30	0.02	1	1	0.29	0.14	0.21	0.24		
	+Y	**4.79**	**3.96**	**4**	**4**	**4**	**1**	**0.04**	**0.15**	**2**	**1**	**0.29**	**0.13**	**0.16**	**0.18**		
	-Y	4.79	3.96	4	4	4	1	0.00	0.15	1	1	0.29	0.24	0.24	0.26		
SVIVA		A	D	D	D	D	A	B		C	A	D	$I_V = 55$			3.90	

5. Conclusions

The present paper deals with the calibration and application of two novel seismic vulnerability assessment methods: (a) Seismic Vulnerability Index for Vernacular Architecture (SVIVA) method; and (b) Seismic Assessment of the Vulnerability of Vernacular Architecture Structures (SAVVAS) method. The calibration of the methods was carried out based on post-earthquake damage data on a set of 88 buildings located in the island of Faial, in Azores, taken from damage drawn up in the sequence of the 1998 earthquake. Since both the main structural features of the buildings and the damage suffered by them are known, it was possible to use that data to calibrate and test the two seismic vulnerability assessment methods, which by itself is a valuable exercise and a major contribution to this field of research.

The availability of post-earthquake damage data has contributed to the main outcome of the paper, which was the calibration and the validation of two new methods as large scale seismic vulnerability assessments for vernacular

architecture. The calibration process was particularly important for the SVIVA method because it led to the adjustment of the analytical expression that correlates the vulnerability index with the mean damage grade. In the case of SAVVAS method, a correlation between the seismic input in terms of PGA and the EMS-98 damage grades was established a priori and then validated using the available damage data. The application of both methods led to very good results in terms of predicted versus observed damage grades, confirming the validity of both methods as first level approaches using few input data, mostly qualitative.

The second main contribution is the first application of the SAVVAS method, which has been recently developed, on a case study. The paper thus has focused on presenting the advantages of this method with respect to other existing methods. Among these advantages, the SAVVAS method shows an enhanced prediction capability. First of all, one of the main advantages of the SAVVAS method is the fact that the correlation between damage and seismic input could be applied directly, while the SVIVA method needed to be calibrated based on the observed results to obtain a good accuracy. Secondly, results were very accurate and showed very low deviations between estimated and observed damage. Since the data used for the application is slightly more specific, it allows a significantly more detailed assessment. The SAVVAS method is able to detect more precisely the differences in the seismic performance of buildings belonging to the same construction typology that were classified with the same vulnerability index according to the SVIVA method. Finally, the method calculates the vulnerability of the building in different directions, which represents a great advantage in accurately assessing the most vulnerable direction and thus detecting the possible deficiencies of the building under evaluation. In several cases, as in the one reported in Section 4.3, the method was indeed able to identify the failure mode suffered by the building.

In summary, the paper validates the applicability of both methods as large scale seismic vulnerability assessment methods. Both of them proved to be able to identify the buildings that are more vulnerable within the whole evaluated set. This is a key issue because this type of methods takes into account possible uncertainties related to the input information collected at the expeditious inspection phase. Therefore, detecting the most vulnerable elements at risk is essential in order to proceed with a more detailed assessment. It should be highlighted that the amount of information required to perform the seismic vulnerability assessment using both methods is the same. However, the capability of the SAVVAS method to evaluate in more detail the seismic behavior of the buildings makes it particularly adequate for defining and optimizing possible structural retrofitting strategies at an urban or

671 regional level. The SAVVAS method do not only highlights the buildings where the biggest efforts should be
672 concentrated on, but also is able to identify weaknesses in the buildings and possible failure mechanisms, which
673 makes it very useful for managing seismic risk on a city or region.

674

675 **References**

676 ATC-13 (1985) Earthquake damage evaluation data for California, Applied Technology Council(ATC), Redwood
677 City, California, USA

678 ATC-40 (1996) Seismic evaluation and retrofit of concrete buildings, Applied Technology Council (ATC),
679 Redwood City, California, USA

680 Azizi-bondarabadi H, Mendes N, Lourenço PB, Sadeghi NH (2016) Empirical seismic vulnerability analysis for
681 masonry buildings based on school buildings survey in Iran, Bulletin of Earthquake Engineering 14(11): 3195-
682 3229

683 Barbat A, EERI M, Yépez Moya F, Canas JA (1996) Damage Scenarios Simulation for Seismic Risk Assessment
684 in Urban Zones, Earthquake Spectra 12 (3): 371-394

685 Benedetti D, Petrini V (1984) Sulla Vulnerabilità Di Edifici in Muratura: Proposta Di Un Metodo Di Valutazione,
686 L'industria delle Costruzioni 149 (1): 66-74

687 Bilal M, Askan A (2014) Relationships between felt intensity and recorded ground-motion parameters for Turkey,
688 Bulletin of Seismological Society of America 104 (1): 484-496

689 Blondet M, Villa García GM, Brzev S, Rubiños A (2011) Earthquake-resistant construction of adobe buildings: a
690 tutorial, Earthquake Engineering Research Institute (EERI), Oakland, California, USA

691 Bothara J, Brzev S (2012) A tutorial: improving the seismic performance of stone masonry buildings, Earthquake
692 Engineering Research Institute (EERI), Oakland, California, USA

693 Boukri M, Bensaibi M (2008) Vulnerability Index of Algiers Masonry Buildings, in: Proc. of 14th World
694 Conference on Earthquake Engineering, Beijing, China

695 Braga F, Dolce M, Liberatore O (1982) A statistical study on damaged buildings review of the MSK-76 scale, in:
696 Proc. of the Conference of the European Association of Earthquake Engineering, Athens, Greece

697 Calvi GM (1999) A Displacement-Based Approach for Vulnerability Evaluation of Classes of Buildings, Journal
698 of Earthquake Engineering 3 (3): 411-438

699 Calvi GM, Pinho R, Magenes G, Bommer JJ, Restrepo-Vélez LF, Crowley H (2006) Development of seismic
700 vulnerability assessment methodologies over the past 30 years, ISET Journal of Earthquake Technology 34 (472):
701 75-104

702 Colombi M, Borzi B, Crowley H, Onida M, Meroni F, Pinho R (2008) Deriving vulnerability curves using Italian
703 earthquake damage data, Bulletin of Earthquake Engineering 6(3): 485-504

704 Correia M (2017) Experiences from past for today's challenges, in: The road to sustainable development. Chapter
705 6 – Traditional and generational change, La fábrica, Fundación Contemporánea, Madrid, Spain

706 Costa A (2002) Determination of mechanical properties of traditional masonry walls in dwellings of Faial Island,
707 Azores, Earthquake Engineering and Structural Dynamics 31(7): 1361-1382

708 Costa A, Arêde A (2006) Strengthening of structures damaged by the Azores earthquake of 1998, Construction
709 and Building Materials 20(4): 252-268

710 Costa AA, Arêde A, Costa A, Oliveira CS (2011) In situ cyclic tests on existing stone masonry walls and
711 strengthening solutions, Earthquake Engineering and Structural Dynamics 40(4): 449-471

712 Costa AA, Arêde A, Campos Costa A, Penna A, Costa A (2013) Out-of-plane behaviour of a full scale stone
713 masonry façade. Part 1: specimen and ground motion selection, Earthquake Engineering and Structural Dynamics
714 42: 2081-2095

715 D'Ayala DF, Speranza E (2003) Definition of Collapse Mechanisms and Seismic Vulnerability of Historic
716 Masonry Buildings, Earthquake Spectra 19 (3): 479-509

717 D'Ayala D, Meslem A, Vamvatsikos D, Porter K, Rosetto T, Silva V (2014) Guidelines for analytical vulnerability
718 assessment of low/mid-rise buildings - Methodology, Vulnerability Global Component project

719 Decanini L, Gavarini C, Mollaioli F (1995) Proposta di definizione delle relazioni tra intensità macrosismica e
720 parametri del moto del suolo, Proc. of 7th Convegno Nazionale di Igegneria Sismica in Italia, vol. 1: 63-72

721 Degg MR, Homan J (2005) Earthquake vulnerability in the Middle East, Geography 90 (1): 54-66

722 Di Pasquale G, Orsini G, Romeo RW (2005) New developments in seismic risk assessment in Italy, Bulletin of
723 Earthquake Engineering 3: 101-128

724 Dolce M, Masi A, Marino M, Vona M (2003) Earthquake Damage Scenarios of the Building Stock of Potenza
725 (Southern Italy) Including Site Effects, Bulletin of Earthquake Engineering 1 (1): 115-140

726 Eleftheriadou AK, Karabinis (2011) Development of damage probability matrices based on Greek earthquake
727 damage data, Earthquake Engineering and Engineering Vibration 10(1): 129-141

728 Erberick MA (2008) Generation of fragility curves for Turkish masonry buildings considering inplane failure
729 modes, Earthquake Engineering and Structural Dynamics 37: 387-405

730 Faccioli E, Cauzzi C (2006) Macroseismic intensities for seismic scenarios, estimated from instrumentally based
731 correlations, Proc. of First European conference on earthquake engineering and seismology, Geneva, Switzerland

732 Fajfar P (1999) Capacity spectrum method based on inelastic demand spectra. Earthquake Engineering and
733 Structural Dynamics 28: 979-993

734 Ferreira TM, Vicente R, Varum H (2014) Seismic vulnerability assessment of masonry facade walls:
735 development, application and validation of a new scoring method, Structural Engineering and Mechanics 50 (4)
736 :541-561

737 Ferreira TM, Maio R, Vicente R (2017a) Seismic vulnerability assessment of the old city centre of Horta, Azores:
738 calibration and application of a seismic vulnerability index method, Bulletin of Earthquake Engineering 15 (7):
739 2879-2899

740 Ferreira TM, Maio R, Vicente R (2017b) Analysis of the impact of large scale seismic retrofitting strategies
741 through the application of a vulnerability-based approach on traditional masonry buildings, Earthquake
742 Engineering and Engineering Vibration 16: 329-348

743 Gautam D, Prajapati J, Paterno KV, Bhetwal KK, Neupane P (2016) Disaster resilient vernacular housing
744 technology in Nepal, Geoenvironmental Disasters 3(1)

745 Giovinazzi S, Lagomarsino S (2004) A macroseismic model for the vulnerability assessment of buildings, in Proc.
746 of 13th World Conference on Earthquake Engineering, Vancouver BC, Canada

747 Gómez Capera AA, Alberello D, Gasperini P (2007) Aggiornamento Relazioni fra l'Intensità Macrosismica e
748 PGA, Technical Report, Convenzione INGV-DPC 2004-2006

749 Gómez Capera AA, Locati M, Fiorini E, Bazurro P, Luzi L, Massa M, Puglia R, Santulin M (2015) D3.1.
750 Macroseismic and ground motion: site specific conversion rules. DPC-INGV-S2 Project "Constraining
751 observations into Seismic Hazard", deliverable D3.1

752 Grünthal G (1998) European Macroseismic Scale 1998 (EMS-98), European Seismological Commission,
753 Subcommission on Engineering Seismology. Working Group Macroseismic Scales, Cahiers du Centre Européen
754 de Géodynamique et de Séismologie 15

755 Guagenti E, Petrini V (1989) Il caso delle vecchie costruzioni: verso una legge danni-intensità, in Proc. of 4th
756 Italian National Conference on Earthquake Engineering, pp. 145-153, Milan, Italy

757 HAZUS (1999) HAZUS earthquake loss estimation methodology: technical manual, Vol. 1, Federal Emergency
758 Management Agency (FEMA), Washington D.C., USA

759 Hofer L, Zampieri P, Zanini MA, Faleschini F, Pellegrino C (2018) Seismic damage survey and empirical fragility
760 curves for churches after the August 24, 2016 Central Italy earthquake, Soil Dynamics and Earthquake
761 Engineering 111: 98-109

762 Hyams DG (2017) CurveExpert Professional Documentation, Release 2.6.4., Hyams Development

763 ICOMOS (1999) Charter on the built vernacular heritage, International Council of Monuments and Sites
764 (ICOMOS), ICOMOS 12th General Assembly, Mexico

765 Jaiswal K, Aspinall W, Perkins D, Wald D, Porter KA (2012) Use of expert judgement to estimate seismic
766 vulnerability of selected building types, in: Proc. of 15th World Conference on Earthquake Engineering, Lisbon,
767 Portugal

768 Lagomarsino S, Giovinazzi S (2006) Macroseismic and mechanical models for the vulnerability assessment of
769 current buildings, Bulletin of Earthquake Engineering 4 (4): 415-433

770 Lagomarsino S, Penna A, Galasco A, Cattari S (2013) TREMURI program: An equivalent frame model for the
771 nonlinear seismic analysis of masonry buildings, Engineering Structures 56: 1787-1799

772 Margottini C, Molin D, Serva L (1992) Intensity versus ground motion: a new approach using Italian data,
773 Engineering Geology 33: 45-58

774 Marin S, Avouac JP, Nicolas M, Schlupp A (2004) A probabilistic approach to seismic hazard in metropolitan
775 France, Bulletin of Seismological Society of America 94 (6): 2137-2163

776 Matias L, Dias NA, Morais I, Vales D, Carrilho F, Madeira J, Gaspar JL, Senos L, Silveira AB (2007) The 9th of
777 July 1998 Faial Island (Azores, North Atlantic) seismic sequence, Journal of Seismology 11(3): 275-298

778 May J (2010) Handmade houses & other buildings: the world of vernacular architecture, Thames & Hudson,
779 London, UK

780 Murphy JR, O'Brien LJ (1977) The correlation of peak ground acceleration amplitude with seismic intensity and
781 other physical parameters, Bulletin of Seismological Society of America 67 (3): 877-915

782 Musson R, Grünthal G, Strucchi M (2010) The comparison of macroseismic intensity scales, Journal of
783 Seismology 14(2): 413-428

784 Neves F, Costa A, Vicente R, Oliveira CS, Varum H (2012) Seismic vulnerability assessment and characterization
785 of the buildings on Faial Island, Azores, Bulletin of Earthquake Engineering 10 (1): 27-44

786 Ortega J (2018) Reduction of the seismic vulnerability of vernacular architecture with traditional strengthening
787 solutions, Ph.D. thesis, University of Minho, Guimarães, Portugal

788 Ortega J, Vasconcelos G, Rodrigues H, Correia M, Lourenço PB (2017) Traditional earthquake resistant
789 techniques for vernacular architecture and local seismic cultures: A literature review, Journal of Cultural Heritage
790 27: 181-196

791 Pasticier L, Amadio C, Fragiacomo M (2008) Non-linear seismic analysis and vulnerability evaluation of a
792 masonry building by means of the SAP2000 V. 10 code, Earthquake Engineering and Structural Dynamics 37:
793 467-485

794 Pitilakis K, Crowley H, Kaynia AM (Eds.) (2014) SYNER-G: Typology definition and fragility functions for
795 physical elements at seismic risk. Buildings, lifelines, transportation networks and critical facilities. Series:
796 Geotechnical, geological and earthquake engineering (GGEE), vol. 27, Springer

797 Rossetto T, Iaoannou I, Grant DN (2015) Existing empirical fragility and vulnerability functions: Compendium
798 and guide for selection, GEM Technical Report 2015-1

799 Rota M, Penna A, Strobbia C (2006) Typological Fragility Curves from Italian Earthquake Damage Data, in:
800 Proc. of First European Conference on Earthquake Engineering and Seismology, Geneva, Switzerland

801 Rota M, Penna A, Magenes G (2010) A methodology for deriving analytical fragility curves for masonry buildings
802 based on stochastic nonlinear analyses, Engineering Structures 32: 1312-1323

803 Sabetta F, Goretti A, Lucantoni A (1998) Empirical Fragility Curves from Damage Surveys and Estimated Strong
804 Ground Motion, in: Proc. of 11th European Conference on Earthquake Engineering, Paris, France

805 Sepe V, Speranza E, Viskovic A (2008) A method for large-scale vulnerability assessment of historic towers,
806 Journal of Structural Control and Health Monitoring 15: 389-415

807 Silva V, Akkar S, Baker J, Bazzurro P, Castro JM, Crowley H, Dolsek M, Galasso C, Lagomarsino S, Monteiro
808 R, Perrone D, Pitilakis K, Vamvatsikos D (2019) Current challenges and future trends in analytical fragility and
809 vulnerability modelling, Earthquake Spectra

810 Shakya M (2014) Seismic vulnerability assessment of slender masonry structures, Ph.D. thesis, Universidade de
811 Aveiro, Aveiro, Portugal

812 Sorrentino L, Liberatore L, Liberatore D, Masiani R (2013) The behaviour of vernacular buildings in the 2012
813 Emilia earthquakes, Bulletin of Earthquake Engineering 12(5): 2367-2382

814 Spence RJS, Coburn AW, Pomonis A, Sakai S (1992) Correlation of ground motion with building damage: The
815 definition of a new damage-based seismic intensity scale, in: Proc. of 10th Conference on Earthquake Engineering,
816 Madrid, Spain

817 Theodulis NP, Papazachos BC (1992) Dependence of strong ground motion on magnitude distance, site geology
818 and macroseismic intensity for shallow earthquake in Greece: I, peak horizontal acceleration, velocity and
819 displacement, Soil Dynamics and Earthquake Engineering 11: 387-402

820 Tselentis GA, Danciu L (2008) Empirical relationships between modified Mercalli intensity and engineering
821 ground-motion parameters in Greece, Bulletin of Seismological Society of America 98 (4): 1863-1875

822 Vicente R (2008) Estratégias e metodologias para intervenções de reabilitação urbana. Avaliação da
823 vulnerabilidade e do risco sísmico do edificado da Baixa de Coimbra, Ph.D. thesis, Universidade do Aveiro,
824 Aveiro, Portugal

825 Vicente R, Parodi S, Lagomarsino S, Varum H, Mendes da Silva JAR (2011) Seismic vulnerability and risk
826 assessment: a case study of the historic city centre of Coimbra, Portugal, Bulletin of Earthquake Engineering 9
827 (4): 1067-1096

828 Wald DJ, Quitoriano V, Heaton TH, Kanamori H (1999) Relationships between peak ground acceleration, peak
829 ground velocity and modified Mercalli intensity in California, Earthquake Spectra 15: 557-564

830 Whitman RV, Reed JW, Hong ST (1974) Earthquake Damage Probability Matrices, in: Proc. of the 5th World
831 Conference on Earthquake Engineering, Rome, Italy

832 Zampieri P, Zanini MA, Faleschini F (2016) Derivation of analytical seismic fragility functions for common
833 masonry bridge types: methodology and application to real cases, Engineering Failure Analysis 68: 275-291

834 Zanini MA, Hofer L, Faleschini F, Pellegrino C (2017) The influence of record selection in assessing uncertainty
835 of failure rates, Ingegneria Sismica 34(4): 30-40

836 Zanini MA, Hofer L, Faleschini F (2019) Reversible ground motion-to-intensity conversion equations based on
837 the EMS-98 scale, Engineering Structures 180: 310-320

838 Zonno G, Oliveira CS, Ferreira MA, Musacchio G, Meroni F, Mota-de-Sá F, Neves F (2010) Assessing seismic
839 damage through stochastic simulation of ground shaking: The case of 1998 Faial earthquake (Azores Islands),
840 Surveys in Geophysics 31(3): 361-381

841

842